

Structural and electro-optic properties of $\text{Ba}_{0.7}\text{Sr}_{0.3}\text{TiO}_3$ thin films grown on various substrates using pulsed laser deposition

D. Y. Wang,^{a)} J. Wang, H. L. W. Chan, and C. L. Choy

Department of Applied Physics and Materials Research Centre, The Hong Kong Polytechnic University, Hong Kong, China

(Received 18 October 2006; accepted 30 December 2006; published online 23 February 2007)

Epitaxial $\text{Ba}_{0.7}\text{Sr}_{0.3}\text{TiO}_3$ (BST) thin films were deposited on various single crystal substrates, including LaAlO_3 (LAO) (001), $(\text{LaAlO}_3)_{0.3}(\text{Sr}_2\text{AlTaO}_6)_{0.35}$ (LSAT) (001), and SrTiO_3 (STO) (001), using pulsed laser deposition in order to study their structural and electro-optic properties. All the films exhibit a good crystalline quality and a pure perovskite phase with a distorted lattice structure. The in-plane temperature dependence of relative permittivity of the films was measured on interdigital electrodes. The films grown on LAO and LSAT exhibited an obvious room-temperature ferroelectric state, while the film grown on STO showed a broad phase transition peak near room temperature. Correspondingly, large linear electro-optic effects were observed in the BST films grown on LAO and LSAT in a transverse geometry at a wavelength of 632.8 nm using a modified Sénarmont method. The linear electro-optic coefficient r_c of the BST films grown on LAO and LSAT was found to be 82.7×10^{-12} and 125.0×10^{-12} m/V, respectively. Nevertheless, a predominantly quadratic and slightly asymmetric electro-optic behavior is observed for the film grown on STO with the quadratic electro-optic coefficient R_c of 12.9×10^{-18} m^2/V^2 . © 2007 American Institute of Physics. [DOI: 10.1063/1.2646014]

INTRODUCTION

Thin film ferroelectric materials are potentially applicable in various guided-wave optical devices, such as switch or modulator, which control optical signal in an optical integrated circuit.¹ The motivation for using ferroelectric thin films is their excellent electro-optic (EO) properties, which is a critical factor to obtain high device efficiency. The use of thin film ferroelectrics in EO devices offers several advantages over bulk materials such as lower driving voltages, higher modulation speeds, and the potential for monolithic integration.² Great efforts have been made to find suitable ferroelectric oxide materials that have large EO coefficients and can be epitaxially deposited on suitable substrates. To date, the most widely studied ferroelectrics for EO applications are the niobates and titanates, including LiNbO_3 ,³ $\text{Sr}_x\text{Ba}_{1-x}\text{Nb}_2\text{O}_6$,⁴ KNbO_3 ,⁵ $(\text{Pb},\text{La})(\text{Zr},\text{Ti})\text{O}_3$,⁶ BaTiO_3 ,⁷ $(1-x)\text{Pb}(\text{Mg}_{1/3}\text{Nb}_{2/3})\text{O}_3-x\text{PbTiO}_3$,⁸ etc. Recently, the deposition of ferroelectric oxide thin films by a variety of techniques has been explored including molecular beam epitaxy (MBE), pulsed laser deposition (PLD), sputtering, sol-gel, and metal-organic chemical vapor deposition (MOCVD). In contrast to other methods, PLD permits a stoichiometric transfer of material from the target to the film and film growth at high temperatures in reactive ambient gas, in particular, oxygen. $\text{Ba}_{1-x}\text{Sr}_x\text{TiO}_3$, abbreviated as BST, traditionally considered as an excellent microwave material for wide applications in wireless communication due to its large dielectric tenability at gigahertz, attracts much attention in optoelectronic community since the discovery of high EO coefficients in PLD-produced $\text{Ba}_{1-x}\text{Sr}_x\text{TiO}_3$ thin films in the year 2000.^{9,10}

For integration, films are not only required to have EO properties comparable to those of the bulk but must also have a high degree of microstructure perfection in order to minimize optical scattering losses since the optical signal must survive after passing through such devices. The optical propagation loss has been the most serious barrier for practical applications of ferroelectric thin films to waveguide devices. Hence it must be reduced below a level of about 1 dB/cm for practical applications.¹¹ BST thin films have been proved to possess acceptable loss in our previous work.¹² Thus BST was considered to be a very promising candidate for active waveguide applications.

Although the EO properties of bulk ferroelectric materials, such as single crystals of LiNbO_3 and BaTiO_3 , and $(\text{Pb},\text{La})(\text{Ti},\text{Zr})\text{O}_3$ transparent ceramics, are well identified, the identification of the EO properties of ferroelectric thin films is not easy since they exhibit process-dependent properties.¹³ In addition, substrate can effectively modify the structure of the ferroelectric thin films,^{14,15} thus the EO properties. Crystals with a noncentrosymmetric structure exhibit a predominantly linear electro-optic behavior while crystals with a centrosymmetric structure show a quadratic EO effect. It is known that $\text{Ba}_{1-x}\text{Sr}_x\text{TiO}_3$ transforms from the ferroelectric phase to the paraelectric phase at the Curie temperature (T_c), at which the structure changes from tetragonal to cubic. Therefore, the knowledge of structure and ferroelectric state at room temperature may lead to a better understanding of the EO behavior in $\text{Ba}_{1-x}\text{Sr}_x\text{TiO}_3$ thin films.

In this work, $\text{Ba}_{0.7}\text{Sr}_{0.3}\text{TiO}_3$ thin films were epitaxially grown on various substrates, including LaAlO_3 (001) [abbreviated as LAO (001)], $(\text{LaAlO}_3)_{0.3}(\text{Sr}_2\text{AlTaO}_6)_{0.35}$ (001) [abbreviated as LSAT (001)], and SrTiO_3 (001) [abbreviated as STO (001)], using PLD in order to study the substrate effect

^{a)}Electronic mail: apdywang@polyu.edu.hk

TABLE I. PLD conditions of $\text{Ba}_{0.7}\text{Sr}_{0.3}\text{TiO}_3$ thin films.

Target-substrate distance	50 mm
Laser energy	250 mJ
Repetition rate of pulsed laser	10 Hz
Ambient gas	O_2
Total pressure of ambient gas	27 Pa
Substrate temperature	750 °C
Growth rate	~ 20 nm/min

on the structural and EO properties of BST thin films, and their EO behaviors were explained incorporated with their room-temperature ferroelectric state.

EXPERIMENTS

PLD technique was employed in this study to produce epitaxial $\text{Ba}_{0.7}\text{Sr}_{0.3}\text{TiO}_3$ thin films. $\text{Ba}_{0.7}\text{Sr}_{0.3}\text{TiO}_3$ films of approximately 600 nm thickness were grown on LAO (001), LSAT (001), and STO (001) single crystal substrates polished on both sides by irradiating the stoichiometric target with a laser beam of 248 nm wavelength and 25 ns pulse duration from a KrF excimer laser (Lambda Physik COMPex 250). The pulse energy of the laser beam was 250 mJ and the repetition rate was 10 Hz. The distance between the target and the substrates was fixed at 50 mm. The substrate temperature was maintained at 750 °C. The oxygen partial pressure was kept at 27 Pa during the laser ablation process. The PLD conditions are summarized in Table I. After deposition, the films were postannealed at 1000 °C in a tube furnace for 3 h. The crystal structures of the $\text{Ba}_{0.7}\text{Sr}_{0.3}\text{TiO}_3$ thin films were examined using an x-ray diffractometer (Bruker D8 Discover) equipped with $\text{Cu K}\alpha$ radiation.

The temperature dependence of dielectric permittivity of the thin films was determined along an in-plane direction on an interdigital electrode capacitor (IDEC) with a configuration of electrode/BST/substrate. The top Au interdigital electrodes (IDEs) were deposited by rf magnetron sputtering and patterned by photolithography and wet chemical etching techniques. The IDE has a total of 21 fingers with the finger length of 925 μm and finger width of 5 μm . The finger spacing is 3 μm . The IDE was wire bonded to a piece of Printed Circuit Board (PCB) for easy handling and better electrical contact in subsequent measurements. The dielectric properties were measured using an HP 4294A impedance analyzer connected to a temperature controlled chamber (Oxford). The calculation from the capacitance of the film to obtain the dielectric constant was conducted by using a MATHEMATICA program developed based on Gevorgian's model,^{16,17} which has established the relationship between the capacitance and the electrode size and the material properties.

RESULTS AND DISCUSSIONS

Figure 1 shows the typical $\theta/2\theta$ x-ray diffraction (XRD) patterns of the $\text{Ba}_{0.7}\text{Sr}_{0.3}\text{TiO}_3$ thin films. Only strong (00 l) peaks appear in the XRD patterns, which imply that all the BST thin films have a pure perovskite phase. The in-plane alignment of the BST thin films with respect to the major

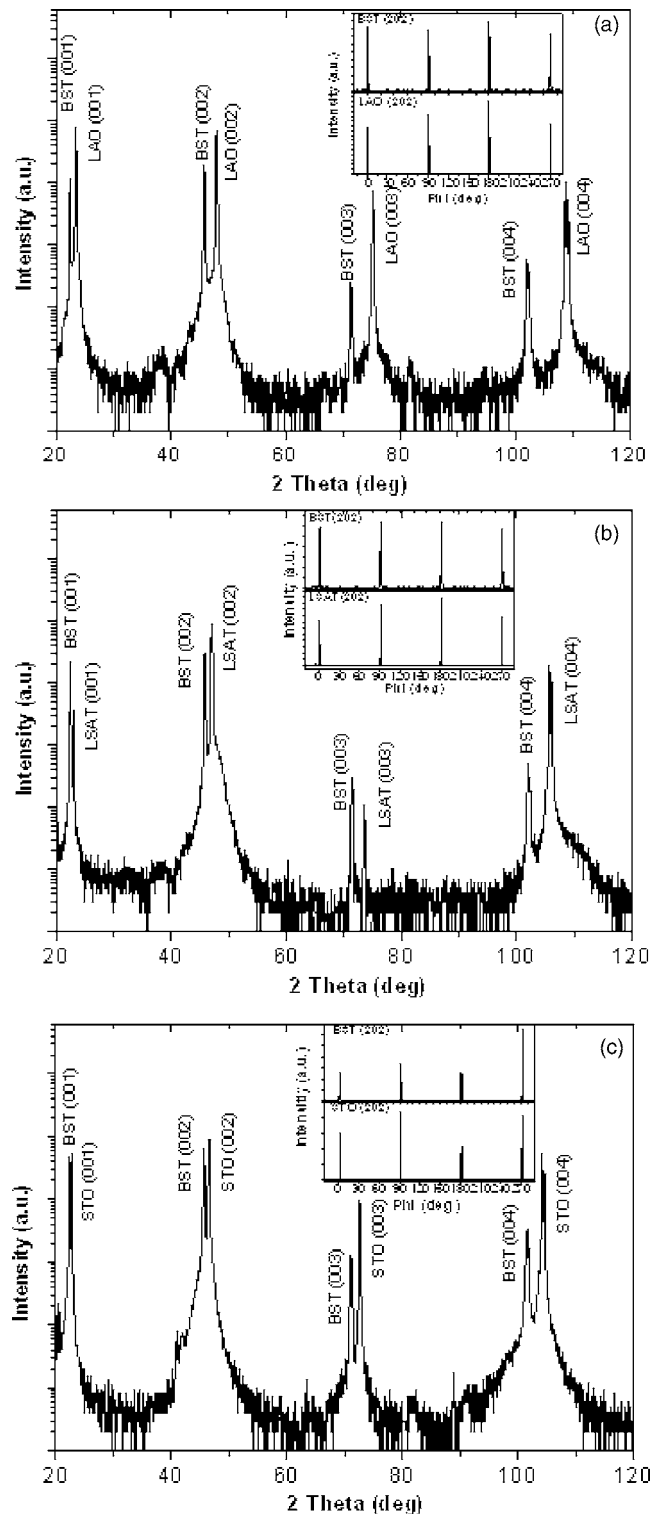


FIG. 1. XRD $\theta/2\theta$ scan patterns of the $\text{Ba}_{0.7}\text{Sr}_{0.3}\text{TiO}_3$ thin films grown on (a) LAO (001), (b) LSAT (001), and (c) STO (001) substrates. The insets show φ scans of the $\text{Ba}_{0.7}\text{Sr}_{0.3}\text{TiO}_3$ (202) and substrate (202) reflections.

axes of the (001) substrates was also confirmed by the XRD off-axis φ scan of the BST (202) and substrate (202) reflections, as shown in the insets of Fig. 1, indicating an epitaxial growth of the BST thin films. Optical loss in optical devices originated from various structure defects, such as point defects, grain boundaries, misorientation, and surface roughness. Hence, fabrication of structural defect-free films, epi-

TABLE II. Lattice parameters of $\text{Ba}_{0.7}\text{Sr}_{0.3}\text{TiO}_3$ thin films on various substrates at room temperature.

Substrate	Crystal structure	Lattice parameters (\AA)			FWHM of rocking curve of BST (002) peak (deg)
		Substrate	Out of plane c	In plane a	
LAO	Rhombohedral	3.780	3.9702	4.0191	0.13
LSAT	Cubic	3.868	3.9706	3.9967	0.14
STO	Cubic	3.901	3.9796	3.9365	0.12
$\text{Ba}_{0.7}\text{Sr}_{0.3}\text{TiO}_3$ bulk ceramics	Cubic		3.970		NA

taxial of single crystalline thin films, is required for optical waveguide devices. Besides, epitaxy is necessary if the ferroelectric thin film is to have EO properties comparable to the bulk.^{11,18}

The rocking curve measurements of the BST (002) reflections revealed that the full width at half maximum (FWHM) values are about 0.13° , 0.14° , and 0.12° for the films grown on LAO, LSAT, and STO substrates, respectively, which indicate that the crystallites are fairly well ordered. Lattice parameters were determined from the XRD results. The lattice spacings d_{002} and d_{202} were calculated, and then the out-of-plane lattice parameter c ($=2d_{002}$) and the in-plane lattice parameter $a=(2/\sqrt{d_{202}^{-2}-d_{002}^{-2}})$ were derived.¹⁹ The in-plane and out-of-plane lattice parameters are shown in Table II. It is seen that all the films have a tetragonal structure, which is different from that of the bulk ceramics, indicating that structures of the films have been modified by the substrates. The film grown on STO (001) substrate has a shortened in-plane lattice parameter and an elongated out-of-plane lattice parameter. It is reasonable since the STO has a comparatively smaller lattice parameter which may cause a stress, thus the in-plane lattice of BST thin film was compressed, while the out-of-plane lattice was elongated as a result of an elastic deformation of the lattice. Situations for the films grown on LAO and LSAT are similar but more complicated than that of the film grown on STO. The out-of-plane lattices have almost no change but the in-plane lattice parameters have been noticeably elongated. This seems somewhat different from the pure strain effect. Other factor, such as oxygen deficiency, may be responsible for the unusual lattice distortion.²⁰ The lattice mismatch will lead to the contraction of the lattice structure, while the oxygen vacancies lead to the tensile stress due to the fact that oxygen vacancies affect the nearest neighbor distance by reducing the Coulombic attraction between cations and anions. Though the oxygen ambient is used to prevent the formation of oxygen vacancies in the deposited film, it has been shown that oxide films grown using PLD are still oxygen deficient.²¹ In our case, oxygen deficiency is presumably the dominant factor that affects the lattice distortion.

$\text{Ba}_{1-x}\text{Sr}_x\text{TiO}_3$ thin films exhibit different dielectric and ferroelectric behaviors when grown on different substrates.^{22,23} Substrates can modify the physical properties of thin films via the strains induced by the lattice misfit or difference in thermal expansion between the film and the substrate. As a result, the properties of the thin films can be

markedly different than the intrinsic properties of the corresponding unstrained bulk materials.^{24–26} Although such strain sometimes leads to degraded film properties, if judicious use is made of substrates and growth parameters, strain offers the opportunity to enhance particular properties of a chosen material in thin film form, and this is called “strain engineering.” Strain engineering is a very hot topic in state-of-the-art thin film studies, since strain is an effective way to adjust the Curie temperature of ferroelectric thin films. Figure 2 shows the temperature-dependent in-plane relative permittivity ϵ of the BST thin films. The curves for films grown on LAO and LSAT exhibit a maximum in ϵ at $T_C=80$ and 105°C , respectively, which are higher than that of bulk $\text{Ba}_{0.7}\text{Sr}_{0.3}\text{TiO}_3$ ceramics ($T_C=35^\circ\text{C}$).²⁷ The upward shift of T_C in the BST thin films along the in-plane direction is believed to be due to the elongation of the in-plane lattice parameter. In general, if there is a tensile stress along the in-plane direction inside the film, then the Curie temperature of the BST thin films is likely to shift towards the high temperature direction. Conversely, a compressive stress may lower the Curie temperature of the films. The film grown on STO shows a broadened ϵ - T curve with the Curie temperature at 40°C , as shown in Fig. 2(c), which is almost the same as that of bulk $\text{Ba}_{0.7}\text{Sr}_{0.3}\text{TiO}_3$ ceramics. Broadening of the ϵ - T curve is presumably due to the diffusion of the STO substrate into BST near the film-substrate interface, thus a layer of “gradient” BST thin film was formed near the interface. The measurements of ϵ - T confirm that films deposited on LAO and LSAT substrates show significant ferroelectric activity at room temperature because their Curie temperatures have shifted to temperatures much higher than room temperature. However, the film grown on STO substrate has a Curie point close to room temperature and exhibits very ferroelectric activity at room temperature. Insets of Fig. 2 are the hysteresis loops of BST films measured at room temperature, which can give more evidence of the room-temperature ferroelectric state in BST films. Knowledge of whether the BST thin film is in the ferroelectric state at room temperature may help us understand its EO behavior.

The EO properties of the BST thin films were measured using a modified Sénarmont method. The electrode pattern used for EO characterization consisted of two coplanar electrodes, with dimensions of $1.0\times 8.0\text{ mm}^2$ separated by a $20\text{-}\mu\text{m}$ -wide gap. The experimental arrangement for the EO measurement is illustrated in Fig. 3. The thin film to be investigated was mounted on a sample holder. The light beam

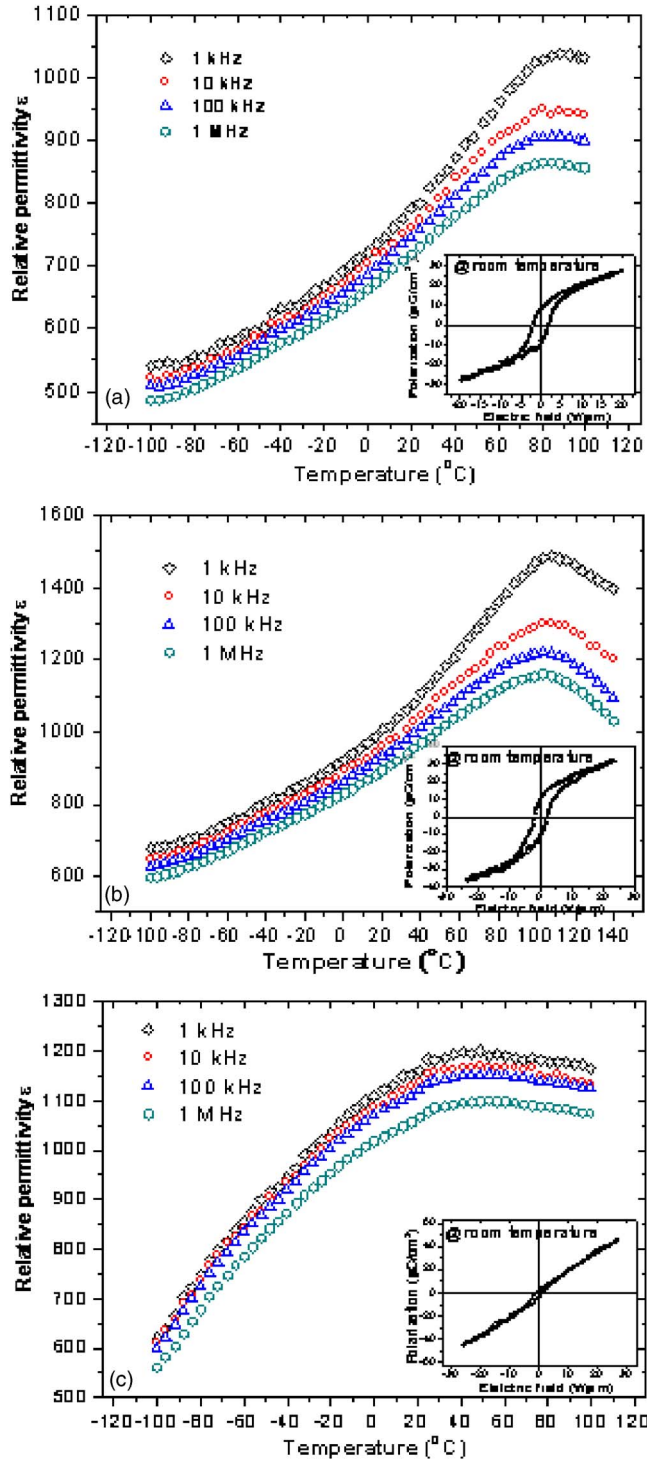


FIG. 2. (Color online) Temperature dependence of the dielectric permittivity of the $\text{Ba}_{0.7}\text{Sr}_{0.3}\text{TiO}_3$ thin films grown on (a) LAO (001), (b) LSAT (001), and (c) STO (001) substrates. The insets are hysteresis loops of the $\text{Ba}_{0.7}\text{Sr}_{0.3}\text{TiO}_3$ thin films measured at room temperature.

from a 2 mW stabilized He–Ne laser (Spectra-Physics model 117A, $\lambda=632.8$ nm), after passing through a polarizer set at -45° , impinged normally on the film in the gap ($20\ \mu\text{m}$ wide) between two gold electrodes. The laser beam was then modulated at 50 kHz by the PEM-90 photoelastic modulator and then passed through an analyzer set at $+45^\circ$. The transmitted laser beam was detected by a photomultiplier tube (PMT). The electrical signal from the PMT was filtered by a

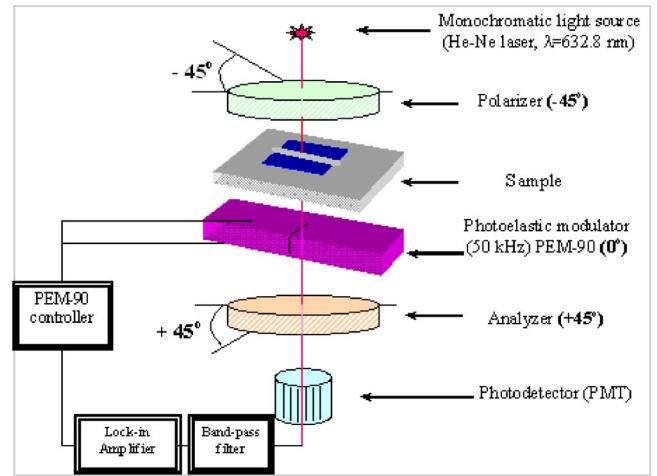


FIG. 3. (Color online) Schematic diagram showing the modified Sénarmont method for the measuring EO coefficients of thin films.

bandpass filter and then fed to a SRS SR830 DSP lock-in amplifier. An electric field was then applied. The general expression for the light intensity I at the detector is given by

$$I = 1 - \cos(B)\cos(A) + \sin(B)\sin(A), \quad (1)$$

where B is the phase retardation in the film sample, and $A = A_0 \cos(\Omega t)$ is the phase retardation in PEM-90 photoelastic modulator. A Fourier series expansion yields

$$I = [1 - \cos(B)J_0(A_0)] + 2 \sin(B)J_1(A_0)\cos(\Omega t) + 2 \cos(B)J_2(A_0)\cos(2\Omega t) + \dots, \quad (2)$$

where $J_n(A_0)$ are the Bessel functions, and the first, second, and third terms represent the dc term, the fundamental term, and the first harmonic term, respectively. Therefore, the electrical signals corresponding to these three terms are

$$V_{dc} = G[1 - \cos(B)J_0(A_0)], \quad (3)$$

$$V_{1(\text{peak})} = 2G \sin(B)J_1(A_0)\cos(\Omega t), \quad (4)$$

$$V_{2(\text{peak})} = 2G \cos(B)J_2(A_0)\cos(2\Omega t), \quad (5)$$

where G is a constant of proportionality. If A_0 is chosen such that $J_0(A_0)=0$, then the dc signal is independent of the sample retardation B . This occurs for $A_0=2.405$ rad. The dc signal may therefore be used to “normalize” the fundamental term

$$\frac{V_{1(\text{peak})}}{V_{dc}} = 2 \sin(B)J_1(A_0). \quad (6)$$

In Eq. (6), $V_{1(\text{peak})}$ is the peak voltage of the signal. However, the lock-in amplifier only gives the rms voltage V_{rms} . For sinusoidal wave forms, V_{rms} is given by

$$V_{\text{rms}} = \frac{V_{(\text{peak})}}{\sqrt{2}}. \quad (7)$$

If we define a ratio R_{1f} as

$$R_{1f} = \frac{V_{1(\text{rms})}}{V_{dc}} = \sqrt{2} \sin(B) J_1(A_0), \quad (8)$$

then the phase retardation B is given by

$$B = \sin^{-1} \left[\frac{R_{1f}}{\sqrt{2} J_1(A_0)} \right] = \sin^{-1} \left[\frac{R_{1f}}{\sqrt{2} J_1(2.405)} \right] \\ = \sin^{-1} \left[\frac{R_{1f}}{\sqrt{2}(0.5191)} \right]. \quad (9)$$

Then the electric field induced birefringence change $\delta(\Delta n)$ can be deduced from the phase change B ,

$$\delta(\Delta n) = \frac{\lambda B}{2\pi t}, \quad (10)$$

where t is the thickness of the film.

Different substrates may result in different EO behaviors even for the same film material, since the room-temperature ferroelectric state of the thin films was modified by the substrate. Using the modified Sénarmont method, the field induced birefringence of the BST thin films was measured as a function of dc electric field E at room temperature and the results are shown in Fig. 4. It is shown that films deposited on LAO and LSAT substrates exhibit predominantly linear birefringence change with respect to dc electric field, which coincide well with its ferroelectric nature. However, a predominantly quadratic and slightly asymmetric EO behavior is observed for the film grown on STO substrate. Generally, the birefringence shift due to linear EO effect (Pockels effect) is given by Eq. (11) and the effective linear electro-optic coefficient r_c can be deduced from the slope of the $\delta\Delta n$ vs E plots. The birefringence shift in a quadratic EO effect (Kerr effect) is given by Eq. (12), from which the effective quadratic electro-optic coefficient R_c can be deduced. The term $1/2n^3R_c$ in Eq. (12) is the slope of the $\delta\Delta n$ vs E^2 plot [Fig. 4(c) inset]. Thus, R_c can be determined if the refractive index n is known.

$$\delta\Delta n = \frac{1}{2} n^3 r_c E, \quad (11)$$

$$\delta\Delta n = \frac{1}{2} n^3 R_c E^2. \quad (12)$$

The effective EO coefficients were calculated and shown in Table III. As shown in Table III, all the films show promising EO properties, showing the potential of BST thin films for use in active waveguide applications. Among them, the best EO properties were found in the films grown on LSAT and STO substrates with $\delta\Delta n$ values of 7.48×10^{-3} and 7.41×10^{-3} , respectively, under a $10 \text{ V}/\mu\text{m}$ dc electric field. The linear EO coefficient r_c of the film grown on LSAT substrate is $125 \times 10^{-12} \text{ m/V}$, which is over six times higher than that of LiNbO_3 single crystal.²⁸ The quadratic EO coefficient R_c of the films grown on STO substrate is $12.9 \times 10^{-18} \text{ m}^2/\text{V}^2$ under the same conditions. It is believed that the good crystalline quality of films grown on LSAT and STO substrates may contribute to their good EO perfor-

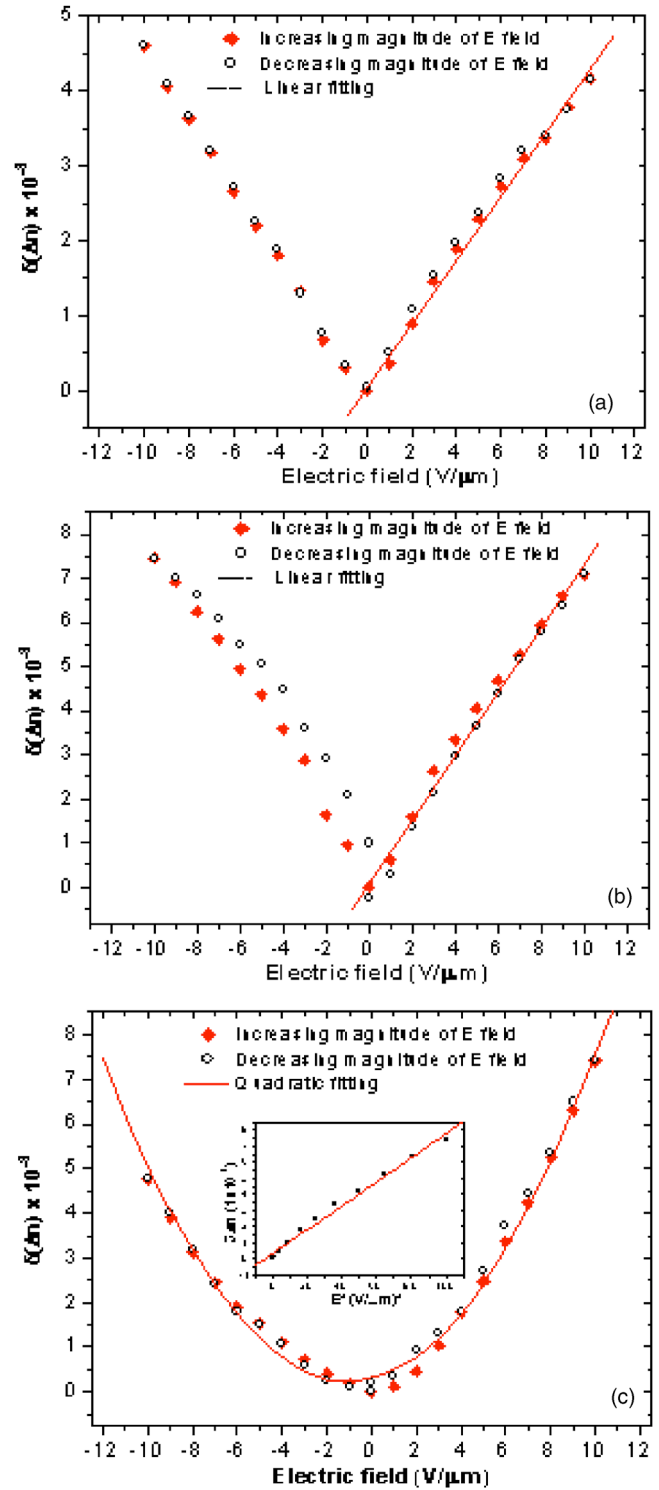


FIG. 4. (Color online) Change in birefringence $\delta(\Delta n)$ as a function of applied dc electric field for $\text{Ba}_{0.7}\text{Sr}_{0.3}\text{TiO}_3$ thin films deposited on (a) LAO (001), (b) LSAT (001), and (c) STO (001) substrates. The inset in (c) shows the $\delta(\Delta n)$ vs E^2 plot.

mance. The presence of twins in films grown on LAO substrates may be an important reason for inferior EO properties.

CONCLUSIONS

In this study, $\text{Ba}_{0.7}\text{Sr}_{0.3}\text{TiO}_3$ thin films have been epitaxially deposited on LAO (001), LSAT (001), and STO (001)

TABLE III. EO properties of $\text{Ba}_{0.7}\text{Sr}_{0.3}\text{TiO}_3$ thin films on various substrates.

Substrate	n at 632.8 nm		Effective EO coefficient		
	Substrate	Film	R_c (10^{-18} m ² /V ²)	r_c (10^{-12} m/V)	$\delta\Delta n(10^{-3})$ at (10 V/ μm) dc
LAO (001)	2.058	2.2858	...	82.7	4.86
LSAT(001)	2.020	2.2820	...	125.0	7.46
STO(001)	2.388	2.2908	12.9	...	7.41
$\text{Ba}_{0.7}\text{Sr}_{0.3}\text{TiO}_3$ bulk ceramics	~2.20	

substrates by pulsed laser deposition. A distorted lattice structure of the thin films was confirmed by x-ray diffraction. The room-temperature ferroelectric state of the thin films was confirmed by the temperature dependence of the dielectric permittivity along the in-plane direction on IDEs. EO properties of the BST films were measured at a wavelength of 632.8 nm through a modified Sénarmont method. It was found that the EO behavior of the thin films was closely related to their room-temperature ferroelectric state. The film grown on STO shows very weak ferroelectric activity at room temperature, thus a quadratic EO behavior appears with the quadratic EO coefficient R_c of 12.9×10^{-18} m²/V². The films deposited on LAO and LSAT show reasonably strong ferroelectric characteristics at room temperature; therefore a linear EO behavior occurs. The linear EO coefficients r_c are 82.7×10^{-12} and 125.0×10^{-12} m/V for the films grown on LAO and LSAT, respectively.

ACKNOWLEDGMENT

Financial support from the Centre for Smart Materials of The Hong Kong Polytechnic University is acknowledged.

¹Y. M. Kang and S. Baik, *J. Mater. Res.* **13**, 995 (1998).

²M. Blomqvist, S. Khartsev, and A. Grishin, *IEEE Photonics Technol. Lett.* **17**, 1638 (2005).

³S. E. Lee, T. W. Noh, and J. H. Lee, *Appl. Phys. Lett.* **68**, 472 (1996).

⁴P. Tayebati, D. Trivedi, and M. Tabat, *Appl. Phys. Lett.* **69**, 1023 (1996).

⁵T. M. Graettinger, S. H. Rou, M. S. Ameen, O. Auciello, and A. I. Kingon, *Appl. Phys. Lett.* **58**, 1964 (1991).

⁶H. Adachi and K. Wasa, *IEEE Trans. Ultrason. Ferroelectr. Freq. Control* **38**, 645 (1991).

⁷D. H. Kim and H. S. Kwok, *Appl. Phys. Lett.* **67**, 1803 (1995).

⁸Y. L. Lu, J. J. Zheng, M. C. Golomb, F. L. Wang, H. Jiang, and J. Zhao,

Appl. Phys. Lett. **74**, 3764 (1999).

⁹J. W. Li, F. Duewer, C. Gao, H. Chang, X. D. Xiang, and Y. L. Lu, *Appl. Phys. Lett.* **76**, 769 (2000).

¹⁰D. Y. Kim, S. E. Moon, E. K. Kim, S. J. Lee, J. J. Choi, and H. E. Kim, *Appl. Phys. Lett.* **82**, 1455 (2003).

¹¹B. W. Wessles, M. J. Nystrom, J. Chen, D. Studebaker, and T. J. Marks, *Mater. Res. Soc. Symp. Proc.* **401**, 211 (1996).

¹²D. Y. Wang, H. L. W. Chan, and C. L. Choy, *Appl. Opt.* **45**, 1972 (2006).

¹³K. Nashimoto, S. Nakamura, T. Morikawa, H. Moriyama, M. Watanabe, and E. Osakabe, *Jpn. J. Appl. Phys., Part 1* **38**, 5641 (1999).

¹⁴H. Adachi, T. Mitsuyu, O. Yamazaki, and K. Wasa, *J. Appl. Phys.* **60**, 736 (1986).

¹⁵M. Gaidi, A. Amassian, M. Chaker, M. Kulishov, and L. Martinu, *Appl. Surf. Sci.* **226**, 347 (2004).

¹⁶Y. Wang, Y. L. Cheng, K. C. Cheng, H. L. W. Chan, and C. L. Choy, *Appl. Phys. Lett.* **85**, 1580 (2004).

¹⁷S. S. Gevorgian, T. Matinsson, P. L. J. Linner and E. L. Kollberg, *IEEE Trans. Microwave Theory Tech.* **44**, 896 (1996).

¹⁸B. W. Wessels, *J. Electroceram.* **13**, 135 (2004).

¹⁹E. D. Specht, H. M. Christen, D. P. Norton, and L. A. Boatner, *Phys. Rev. Lett.* **80**, 4317 (1998).

²⁰N. Navi, H. Kim, J. S. Horwitz, H. D. Wu, and S. B. Qadri, *Appl. Phys. A: Mater. Sci. Process.* **76**, 841 (2003).

²¹W. J. Kim, W. Chang, S. B. Qadri, J. M. Pond, S. W. Kirchoefer, D. B. Chrisey, and J. S. Horwitz, *Appl. Phys. Lett.* **76**, 1185 (2000).

²²C. L. Chen *et al.*, *Appl. Phys. Lett.* **75**, 412 (1999).

²³C. M. Carlson, T. V. Rivkin, P. A. Parilla, J. D. Perkins, D. S. Ginley, A. B. Kozyrev, V. N. Oshadchy, and A. S. Pavlov, *Appl. Phys. Lett.* **76**, 1920 (2000).

²⁴K. J. Choi *et al.*, *Science* **306**, 1005 (2004).

²⁵J. H. Haeni *et al.*, *Nature (London)* **430**, 758 (2004).

²⁶D. Y. Wang, Y. Wang, X. Y. Zhou, H. L. W. Chan, and C. L. Choy, *Appl. Phys. Lett.* **86**, 212904 (2005).

²⁷*Ferroelectrics and Related Substances*, Landolt-Börnstein, New Series, Group III, Vol. 36, edited by H. Landolt (Springer-Verlag, Berlin, 2002), p. 416.

²⁸Y. Xu, *Ferroelectric Materials and Their Applications* (North-Holland, Amsterdam, 1991).

Journal of Applied Physics is copyrighted by the American Institute of Physics (AIP). Redistribution of journal material is subject to the AIP online journal license and/or AIP copyright. For more information, see <http://ojps.aip.org/japo/japcr/jsp>